Molecular Tweezers with Varying Anions: A Comparative Study

ARTICLE *in* THE JOURNAL OF ORGANIC CHEMISTRY · JUNE 2013

Impact Factor: 4.72 · DOI: 10.1021/jo4009673 · Source: PubMed

10 AUTHORS, INCLUDING:

Som Dutt
University of Duisburg-Essen
7 PUBLICATIONS **68** CITATIONS
SEE PROFILE

Thomas Gersthagen
University of Duisburg-Essen
4 PUBLICATIONS **19** CITATIONS
SEE PROFILE

Peter Talbiersky
University of Duisburg-Essen
10 PUBLICATIONS **293** CITATIONS
SEE PROFILE

Matti Hanni
Oulu University Hospital
11 PUBLICATIONS **135** CITATIONS
SEE PROFILE

JOC The Journal of Organic Chemistry

Article

pubs.acs.org/joc

Molecular Tweezers with Varying Anions: A Comparative Study

Som Dutt,[†] Constanze Wilch,[†] Thomas Gersthagen,[†] Peter Talbiersky,[†] Kenny Bravo-Rodriguez,[‡] Matti Hanni,[§] Elsa Sánchez-García,*[,‡] Christian Ochsenfeld,*[,§] Frank-Gerrit Klärner,*[,†] and Thomas Schrader*[,†]

[†]Department of Chemistry, University of Duisburg-Essen, Universitätsstr. 7, 45117 Essen, Germany

[‡]Max-Planck-Institut für Kohlenforschung, Kaiser-Wilhelm-Platz 1, 45470 Mülheim an der Ruhr, Germany

[§]Chair of Theoretical Chemistry, Department of Chemistry, University of Munich (LMU), Butenandtstr. 7, 81377 Munich, Germany and Center for Integrated Protein Science (CIPSM) at the Department of Chemistry, University of Munich (LMU), Butenandtstr. 5-13, 81377 Munich, Germany

Supporting Information

ABSTRACT: Selective binding of the phosphate-substituted molecular tweezer **1a** to protein lysine residues was suggested to explain the inhibition of certain enzymes and the aberrant aggregation of amyloid petide Aβ42 or α-synuclein, which are assumed to be responsible for Alzheimer's and Parkinson's disease, respectively. In this work we systematically investigated the binding of four water-soluble tweezers **1a–d** (substituted by phosphate, methanephosphonate, sulfate, or *O*-methylene-carboxylate groups) to amino acids and peptides containing lysine or arginine residues by using fluorescence spectroscopy, NMR spectroscopy, and isothermal titration calorimetry (ITC). The comparison of the experimental results with theoretical data obtained by a combination of QM/MM and *ab initio* ^{1}H NMR shift calculations provides clear evidence that the tweezers **1a–c** bind the amino acid or peptide guest molecules by threading the lysine or arginine side chain through the tweezers' cavity, whereas in the case of **1d** the guest molecule is preferentially positioned outside the tweezer's cavity. Attractive ionic, CH-π, and hydrophobic interactions are here the major binding forces. The combination of experiment and theory provides deep insight into the host–guest binding modes, a prerequisite to understanding the exciting influence of these tweezers on the aggregation of proteins and the activity of enzymes.

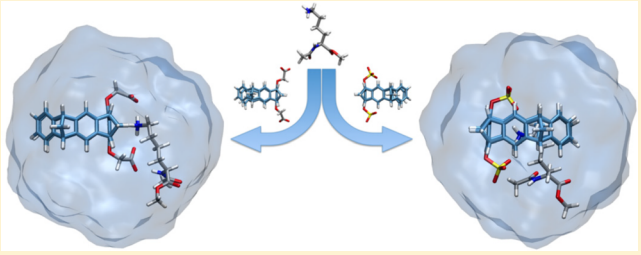

INTRODUCTION

Molecular recognition of specific amino acid residues such as lysine or arginine in peptides and proteins is essential for the regulation of many biological processes such as enzymatic reactions, protein folding, or protein aggregation.[1] Thus, the design and synthesis of water-soluble artificial host molecules, which selectively bind certain amino acids in aqueous solution, represents an important issue of supramolecular chemistry to date. In this respect crown ethers,[2] calixarene derivatives substituted by sulfonate or phosphonate groups,[3] polyanionic cyclophanes,[4] polyaza-arenes ("the arginine cork"),[5] galactose derivatives,[6] and molecular tweezers containing either peptide side chains[7] or porphyrine side walls[8] shall be mentioned here. These compounds serve as host molecules binding lysine and/or arginine derivatives among other amino acid or petide guest molecules, however, with only little selectivity toward one of these guest molecules. Recently, we reported a molecular tweezer bearing lithium methanephosphonate groups in the central benzene bridge (compound **1b** in Figure 1), which binds lysine and its derivatives in buffered aqueous solution at neutral pH more strongly than arginine or histidine by a factor of ca. 2 and 5, respectively. Other amino acids (for example, Asp, Ser, Phe, Leu, Ala, or Gly) are not bound by tweezer **1b**.[9]

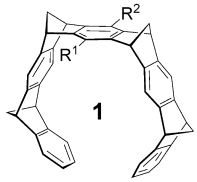

a: $R^1 = R^2 = OPO_3^{2-}\ 2Li^+$
b: $R^1 = R^2 = OP(CH_3)O_2^-\ Li^+$
c: $R^1 = R^2 = OSO_3^-\ Na^+$
d: $R^1 = R^2 = OCH_2CO_2^-\ Na^+$
e: $R^1 = R^2 = OH$
f: $R^1 = R^2 = OAc$
g: $R^1 = R^2 = OCH_2CO_2CH_3$

Figure 1. Structures of molecular tweezers substituted in the central benzene bridge.

The related, also water-soluble, phosphate-substituted tweezer **1a** binds lysine and its derivatives even about 10 times more strongly than the phosphonate tweezer **1b**.[10] Large upfield shifts of the ^{1}H NMR signals assigned to the methylene protons of the lysine or arginine side chain (up to 4 ppm to smaller δ values) were observed for the host–guest complexes of the tweezers **1a** and **1b** with lysine or arginine guest molecules. Due to the magnetic anisotropy of tweezers' arene units these ^{1}H NMR shifts were considered to be an indicator for the threading of the guest side chain into the tweezers' cavity.[9−13]

Received: May 18, 2013
Published: June 10, 2013

dx.doi.org/10.1021/jo4009673 | J. Org. Chem. 2013, 78, 6721−6734

Recently, a single-crystal structure of the complex between phosphate tweezer **1a** and 14-3-3 protein was reported, displaying the threading of a protein lysine side chain through the tweezer's cavity in the crystalline state.[14] **1a** inhibits the enzymatic ethanol oxidation by blocking strategic lysine residues around the active site of the enzyme (alcohol dehydrogenase, ADH).[10] The ability of **1a** to cap critical lysine residues has been also used to prevent the aberrant aggregation of peptides and proteins such as Aβ42 and α-synuclein, which are assumed to be responsible for Alzheimer's and Parkinson's disease, respectively.[11−13]

These remarkable biological effects need to be firmly based on a deep understanding of the mechanistic details of lysine and arginine recognition by these unique receptor molecules. In order to characterize the molecular recognition event, particularly to prove the assumption that these molecular tweezers bind lysine or arginine by threading the positively charged guest side chains through tweezers' cavity, we studied a series of the closely related tweezers **1a−d**, which differed only in the nature of their anions. Using fluorescence and NMR spectroscopy as well as isothermal titration calorimetry (ITC), we elucidated the influence of the different anionic substituents on the molecular recognition of amino acid and peptide guest molecules by these tweezers. The structures of the host−guest complexes were calculated by molecular dynamics simulations (MD) and quantum mechanics/molecular mechanics (QM/MM) methods and subsequently used for quantum chemical *ab initio* calculations of the complexation-induced shifts of the ^{1}H NMR guest signals. The comparison of the theoretical and experimental ^{1}H NMR shift data offers further insight into the host−guest complex structures. This is especially important for the clarification of the already mentioned question of whether the side chain of the lysine or arginine guest molecules is indeed threaded into the tweezers' cavity as was assumed from the experimental ^{1}H NMR data of the previously reported host−guest complexes of the phosphate- and phosphonate-substituted tweezers **1a** and **1b**.[9−11]

RESULTS AND DISCUSSION

Synthesis and Characterization of Tweezers 1a−d. The synthesis of the four tweezers **1a−d** starts from the known hydroquinone tweezer **1e** (Scheme 1).[15] The phosphate- and phosphonate-substituted tweezers **1a** and **1b** were prepared by the reaction of **1e** with $POCl_3$ or $MePOCl_2$ in the presence of triethylamine followed by hydrolysis with dilute HCl and neutralization with LiOH as was already reported.[9,10] The reaction of **1e** with sulfur trioxide pyridinium complex in anhydrous pyridine at 90 °C and subsequent workup with a saturated aqueous solution of $NaHCO_3$ led to the sulfate-substituted tweezer **1c** in an overall yield of 68%. Finally, the carboxylate-substituted tweezer **1d** was prepared by nucleophilic substitution of **1e** with methyl bromoacetate in the presence of potassium carbonate and potassium iodide leading to the tweezer **1g**, followed by hydrolysis of the methylester groups with sodium hydroxide in almost quantitative yield.[16]

The structures of all new compounds were assigned by their spectral data listed in the experimental section of the Supporting Information. The ^{1}H NMR spectra of the phosphate- and sulfate-substituted tweezers **1a** and **1c** are concentration-dependent in aqueous buffer. Particularly, the chemical ^{1}H NMR shifts assigned to the protons attached to the tips of the terminal benzene rings are substantially upfield-shifted (toward smaller δ values) compared to the values measured in CD_3OD, whereas the ^{1}H NMR spectra of the phosphonate- and carboxylate-substituted tweezers **1b** and **1d** are not significantly concentration-dependent. This finding indicates the formation of self-assembled dimers of the tweezers **1a** and **1c** in aqueous solution comparable to the molecular tweezers bearing an extended central naphthalene spacer unit[17] instead of the benzene bridge. The dimerization constants, K_{dim}, and maximum dimerization-induced shifts of the ^{1}H NMR signals of the protons of the tweezers **1a** and **1c** ($\Delta\delta_{max}$) were determined by dilution NMR titration experiments (Table 1).

Scheme 1. Synthesis of Symmetrically Substituted Tweezers 1a−d Starting from Hydroquinone Tweezer 1e

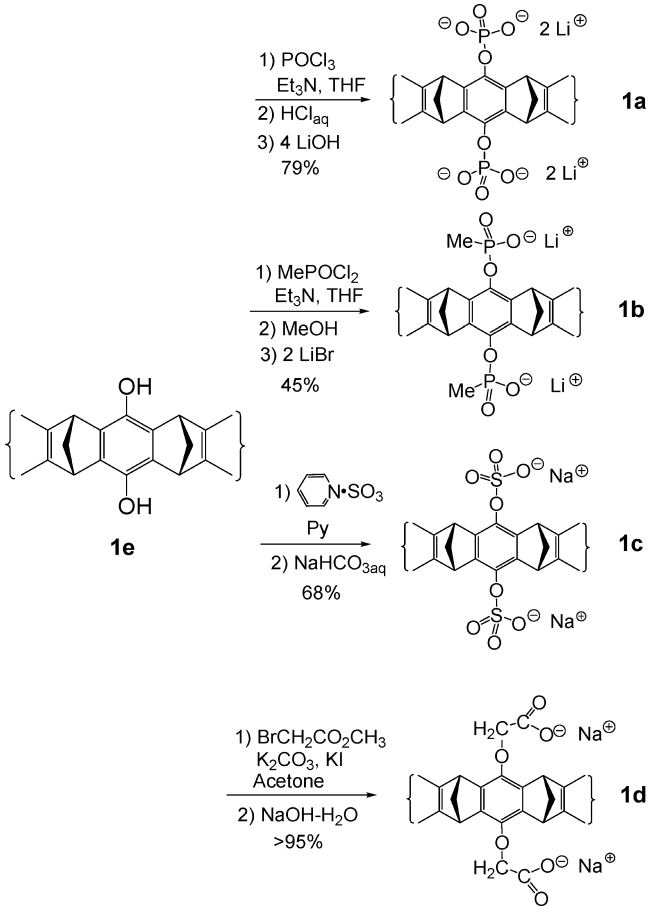

Geometry optimization of the monomers and dimers of tweezers **1a** and **1c** by conformer search using the AMBER*/H_2O force field led to intertwined dimer structures. The calculated dimer structure of the phosphate-substituted tweezer is shown in Table 1 as a representative example. In the structures of the dimers the protons attached to the tips of one tweezer molecule were calculated to point toward the central benzene bridge of the other molecule and experience the magnetic anisotropy of this aromatic ring particularly strongly. These structures are, therefore, in good accord with the observed large upfield shift of ^{1}H NMR signal of the respective protons of $\Delta\delta_{max} \geq 2$ ppm.[18] Contrary to the naphthalene-spaced tweezer, which forms a highly stable dimer ($K_{Dim} = 2.3 \times 10^5$ M^{-1}),[17] the dimers of **1a** and **1c** are only weakly bound (Table 1) and dissociate in dilute solution. Thus, the monomeric tweezers can function as host molecules without paying much energy for the dissociation of their dimers.

dx.doi.org/10.1021/jo4009673 | J. Org. Chem. 2013, 78, 6721−6734

Table 1. Structure of the Dimer [1 (R^1 = R^2 = $O(OH)PO_2^-$)]$_2$, Dimerization Constants K_{Dim} [M^{-1}], and Maximum Dimerization-Induced ^{1}H NMR Shifts $\Delta\delta_{max}$ = $\delta_{dimer} - \delta_{monomer}$ [ppm] of the Protons Attached to the Tips of the Terminal Benzene Rings[a]

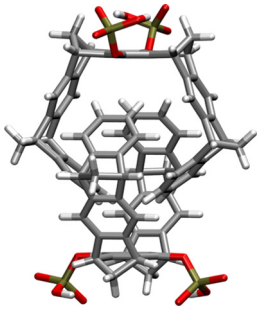

reaction	K_{Dim}	$\Delta\delta_{max}$
2 **1a** → [**1a**]$_2$	60 ± 10	2.2
2 **1c** → [**1c**]$_2$	370 ± 80	2.0
2 **1d** → [**1d**]$_2$	<10	<0.02[b]

[a]Structure of the dimer was calculated by Monte Carlo conformer search (MacroModel, AMBER*/H_2O). Dimerization constants and maximum dimerization-induced ^{1}H NMR shifts were determined by ^{1}H NMR dilution titration experiments in buffered aqueous solution at pH = 7.4 for the molecular tweezers **1a**, **1c**, and **1d** substituted by $OPO_3^{2-}2Li^+$, $OSO_3^-Na^+$, or $OCH_2CO_2^-Na^+$ groups in the central benzene bridge. [b]$\Delta\delta_{obs}$ at the highest measured concentration

Tweezers with a central benzene bridge show a strong emission band at $\lambda_{max} \approx 330$ nm in the fluorescence spectra, which is slightly solvent- and substituent-dependent (**1a**, λ_{max} = 336 nm in H_2O; **1f**, λ_{max} = 318 nm in CH_3CN). The comparison with the spectrum of 1,4-dimethoxybenzene (λ_{max} = 320 nm in CH_3CN) allows the assignment of the tweezers' emission band to the central substituted hydroquinone bridge as chromophor (see Supporting Information, Figure S1). The binding of guest molecules by these tweezers as host molecules leads to partial quenching of this emission band. Thus, the host–guest complex formation can here be detected by fluorescence spectroscopy. The binding constants K_a and hence the dissociation constants K_d ($K_d = 1/K_a$) can be determined by fluorimetric titration experiments.

Characterization of Host–Guest Complexes by Fluorometric and ^{1}H NMR Titration Experiments. N/C-Protected lysine and arginine derivatives were selected as guest molecules besides parent lysine and arginine and small biologically interesting peptides containing either lysine or arginine residues (Figure 2). For example, tripeptide KAA[19] builds bacterial cell walls, KLVFF[20] is the central hydrophobic cluster within the Aβ amyloid peptide sequence, which is discussed as potential nucleation site for pathological protein aggregation, and the pentapeptide KTTKS[21] sends a signal to the injured cell to regenerate its own collagen, with potential applications in anti-aging technology. Another attractive target is the RGD[22] sequence, which constitutes the key recognition element for numerous cell–protein and cell–cell communication events.

The partial quenching of the emission band at λ_{max} = 336 nm of the phosphate tweezer **1a** by successive addition of Ac Lys OMe or Ac Arg OMe as guest molecules in aqueous buffer at pH = 7.6 is shown as a representative example in Figure 3, left column. The quenching is here generally accompanied by a slight blue shift of the emission maximum. However, during the titration of the sulfate tweezer **1c** with peptide KLVFF a new band at λ_{max} = 310 nm appears with increasing intensity, which is even higher at the end of titration than that of the original band of pure **1c** (Figure 3). Since pure KLVFF shows an emission at λ_{max} = 315 nm by itself, this new band at λ_{max} = 310 nm observed for its mixture with **1c** can be certainly assigned to the fluorescence of the adjacent phenylalanine residues of KLVFF. In the titration of the phosphate tweezer **1a** with KLVFF, however, the tweezer's emission is only quenched comparable to all other experiments and no new band appears at shorter wavelength. Evidently, in this case the phenylalanine residues of KLVFF interact with tweezer **1a** leading to the observed quenching of the KLVFF fluorescence contrary to **1c**. (The complete set of all titration experiments is shown in the Supporting Information.)

The binding constants K_a and, hence, the dissociation constants K_d were determined for host–guest complexes of all four tweezers **1a**, **1b**, **1c**, and **1d** with guest molecules containing either lysine or arginine residues (Table 2) by fluorometric titration experiments from the dependencies of the tweezers' emission band on the guest concentration. (For representative examples see Figure 3, right column. The curves of all titration experiments are shown in the Supporting Information).

In buffered aqueous solution at almost neutral pH value, the phosphate-substituted tweezer **1a** is certainly partially protonated, whereas the phosphonate-, sulfate-, and carboxylate-substituted tweezers **1b,c,d** exist as dianions under these conditions. The phosphate tweezer **1a** generally forms more stable host–guest complexes than the sulfate tweezer **1c** followed by the phosphonate and carboxylate tweezers **1b** and **1d**. In addition, the complexes of the lysine derivatives are more stable than those of the corresponding arginine derivatives. The peptides containing two adjacent K units at their *N* terminus (KKLVFF and KKLVFFAK) form the most stable complexes with **1a**. The complex stability is also dependent from the buffer concentration. In more dilute buffered solution (10 mM) the complexes are more stable by a factor of 2–3 than those in solutions containing 200 mM buffer.

The dissociation constants, K_d, were independently determined by ^{1}H NMR titration experiments (Table 3), which are in good agreement with the data determined by fluorometric titration experiments (Table 2). The observed differences in the K_d values are certainly the result of the different concentrations that are necessary for the measurement of the fluorescence and NMR spectra. For the NMR experiments much higher host and guest concentrations are needed than for the fluorescence measurements (mM vs μM). The measurement of the maximum complexation-induced shifts of the ^{1}H NMR guest proton signals, $\Delta\delta_{max}$, provides important information on the host–guest complex structures in addition to the complex stability, which is characterized by the K_d values. In the complexes of the phosphate-, phosphonate-, and sulfate-substituted tweezers **1a–c** large $\Delta\delta_{max}$ values (up to 6 ppm) are observed for the signals of the guest methylene protons assigned to the lysine or arginine side chain. This finding suggests the threading of this side chain through the tweezers' cavity. In the complexes of the carboxylate-substituted tweezer **1d** the $\Delta\delta_{max}$ values of the corresponding guest protons were determined to be substantially smaller ($\Delta\delta_{max}$ < 1 ppm), indicating complex structures different from those of the tweezers **1a–c** (Table 3). To gain further structural information, the structures of the free tweezers, free guest

dx.doi.org/10.1021/jo4009673 | J. Org. Chem. 2013, 78, 6721–6734

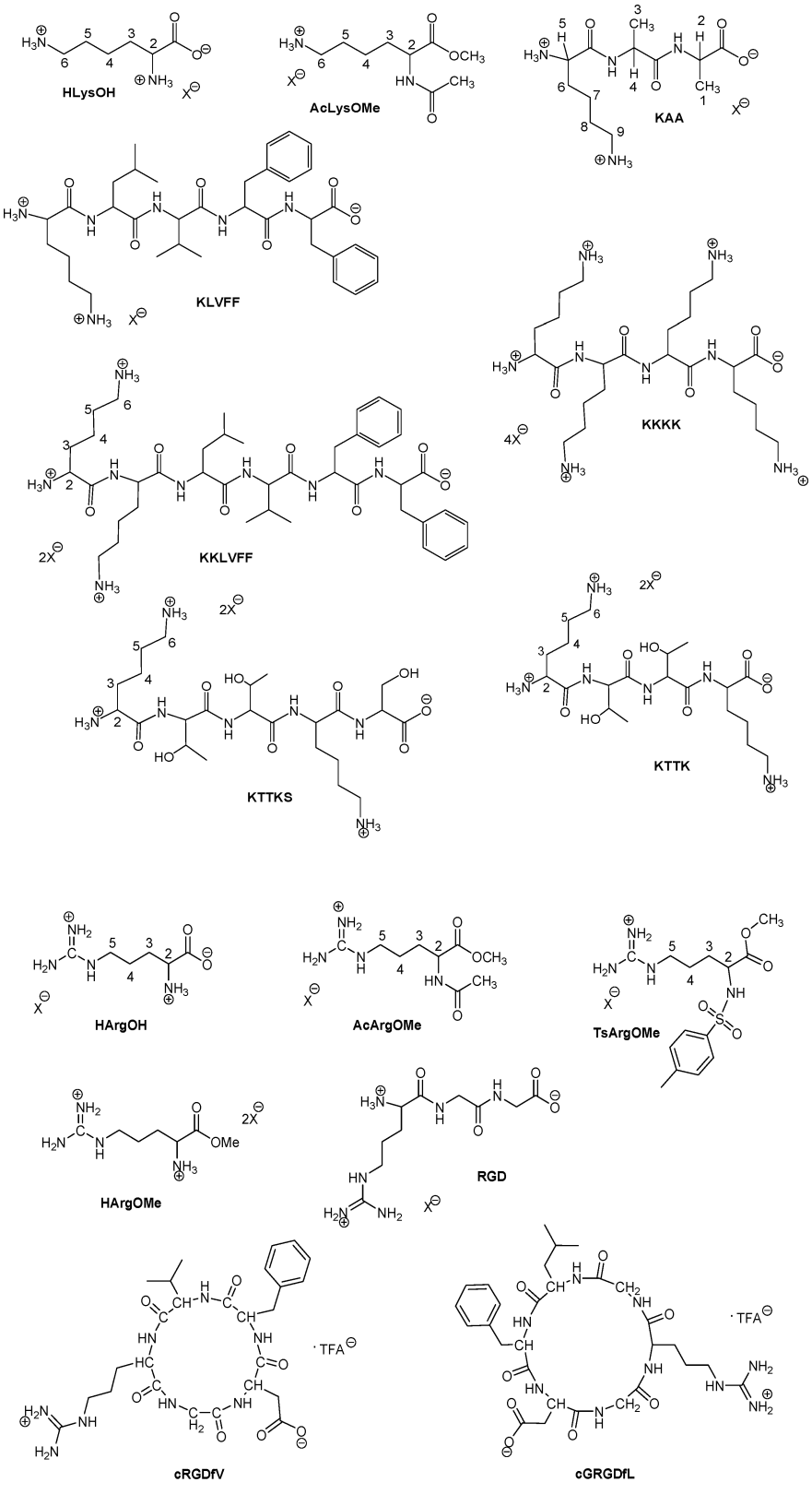

Figure 2. Structures of lysine- and arginine-containing guest molecules (X = Cl).

molecules, and the corresponding host–guest complexes were optimized at the QM/MM level (Figures 5 and 6; Table 5). The resulting complex geometries were subsequently used for ^{1}H NMR shift calculations by the use of quantum chemical *ab initio* methods. The comparison of the experimental and calculated ^{1}H NMR shift data provides good evidence for the host–guest complex structures.

Computation of Host–Guest Complex Structures by QM/MM Methods and of Chemical ^{1}H NMR Shifts by Quantum Chemical *ab Initio* Methods. The monomers and

dx.doi.org/10.1021/jo4009673 | J. Org. Chem. 2013, 78, 6721–6734

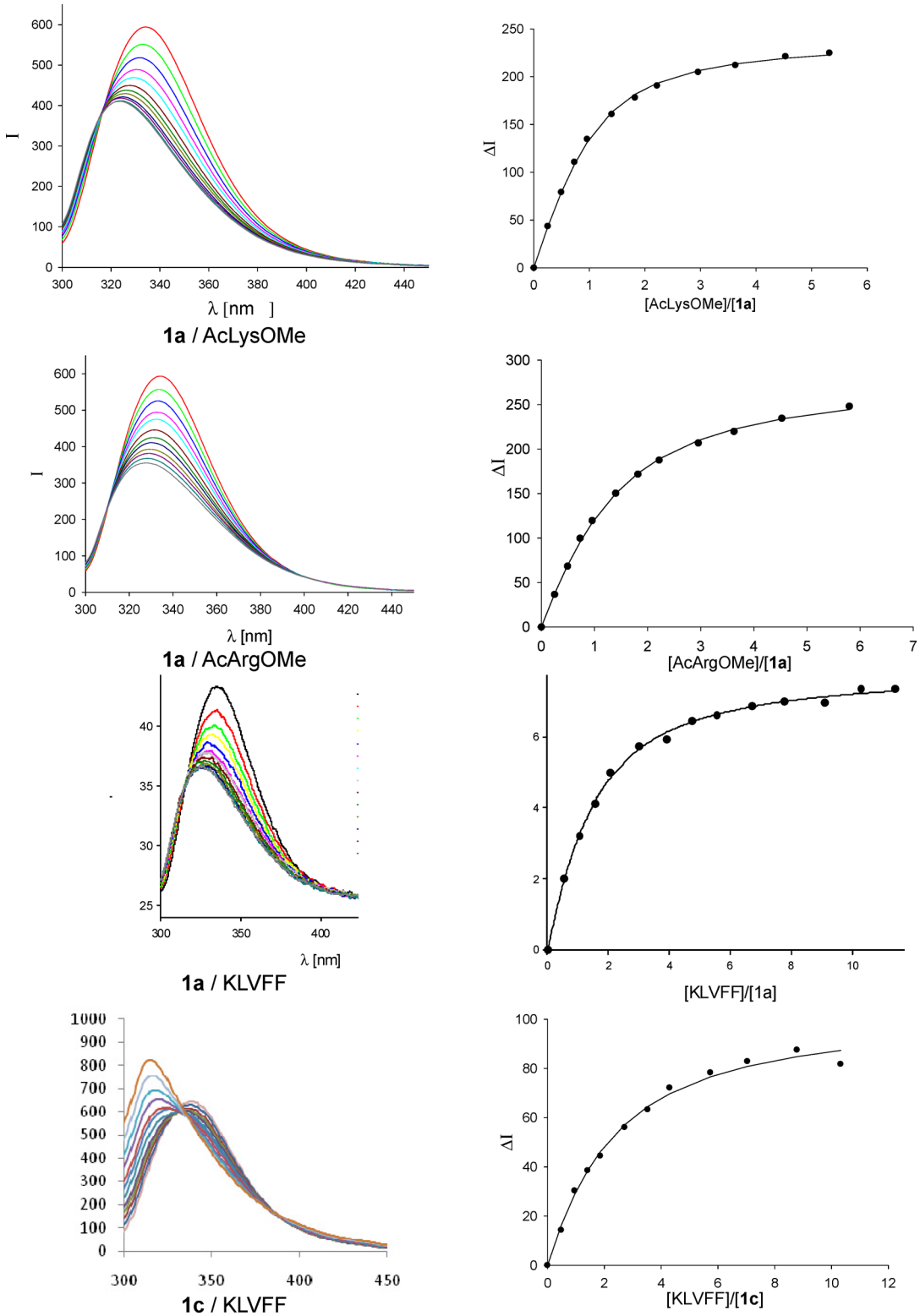

Figure 3. Selected dependencies of the emission band at λ_{em} = 336 nm of the tweezers **1a** and **1c** (λ_{exc} = 285 nm) on the guest concentration in aqueous phosphate buffer (10 mM, pH = 7.6).

the inclusion complexes of the anionic tweezers **1a′−d′** (Figure 5, structures of **1a−d** calculated without the positive counterions) with amino acids or short peptides were investigated using MD simulations and QM/MM calculations. MD simulations were done using the CHARMM c33b1 program with the CHARMM22 force field and the TIP3P model for water.[23−25] Since the phosphate tweezer **1a** is partially protonated in buffered aqueous solution at almost neutral pH value, the mono- and diprotonated structures **1a′** and **1a″**, respectively, were used for the calculation of this system. Snapshots from the MD simulations were optimized at the QM(B3LYP-D2/SVP)/CHARMM level of theory using the

dx.doi.org/10.1021/jo4009673 | J. Org. Chem. 2013, 78, 6721−6734

Table 2. Dissociation Constants K_d [μM] of Host–Guest Complexes of Tweezers 1a, 1b, 1c, and 1d with Lysine- or Arginine-Containing Amino Acid and Peptide Derivatives[a]

guest	1a	1b	1c	1d
Ac Lys OMe	17 ± 6[b,e]	68 ± 1[b]	28 ± 2[b]	226 ± 14[b]
	9 ± 6[c]		19 ± 3[d]	643 ± 7[d]
H Lys OH	21 ± 4[b,e]	874 ± 1[b]	227 ± 6[c]	1170 ± 20[d]
KAA	30 ± 3[b]	905 ± 1[b]	303 ± 5[c]	33333 ± 83[d]
KLVFF	20 ± 5[b]		38 ± 11[c]	
KKLVFF	4 ± 1[b]	71 ± 1[b]		
KKLVFFAK	7 ± 1[b]			
KKKK	10 ± 7[b,]			
Ac Arg OMe	60 ± 2[b]		178 ± 4[b]	882 ± 26[b]
	20 ± 5[c]		77 ± 5[d]	281 ± 18[d]
H Arg OH			699 ± 15[c]	609 ± 27[d]
H Arg OMe			160 ± 6[c]	
RGD	86 ± 1[b]			
cRGDfV	59 ± 11[c]			
cGRGDfL	26 ± 8[c]			

[a]Dissociation constants were determined by fluorometric titration experiments in aqueous phosphate buffer. The standard deviation of K_d is given in [%] of the determined value of K_d. [b]Phosphate buffer, 200 mM, pH = 7.6. [c]Phosphate buffer, 10 mM pH = 7.6. [d]Phosphate buffer, 10 mM, pH = 7.2. [e]Reference 10.

Table 3. Dissociation constants K_d and Maximum Complexation-Induced ^{1}H NMR Shifts of Guest Protons $\Delta\delta_{max} = \delta_{0,G} - \delta_{C,G}$ Determined for Host–Guest Complexes of the Phosphate-, Phosphonate-, Sulfate-, and OCH_2-Carboxylate-Substituted Tweezers 1a, 1b, 1c, and 1d with Lysine- or Arginine-Containing Amino Acid and Peptide Derivatives[a]

host–guest complex	K_d [μM]	$\Delta\delta_{max}$ [ppm]
1a·Ac Lys OMe	17 ± 0	3.91 (6-H), 0.51 (2-H), −0.32 ($NCOCH_3$)
1a·H Lys OH	40 ± 7	4.51 (6-H), 4.47 (5-H), 0.76 (3-H), 0.24 (2-H)
1a·KAA	11 ± 9	5.82, 5.92 (9-H)[b], 3.22 (8-H), 2.28 (7-H)
1a·Ac Arg OMe	22 ± 4	3.75 (5-H), 2.54 (4-H), 1.23 (3-H), 0.63 (2-H)
1b·Ac Lys OMe	227 ± 22[d]	>4 (6-H)[c], 1.45, 1.57 (5-H)[b], 0.57 (2-H)
1b·H Lys OH	714 ± 8[d]	>4 (6-H)[c]
1b·KAA	833 ± 14[d]	2.80 (6-H), 1.03 (5-H), 0.29 (2-H)
$(\mathbf{1b})_2$·KTTK	147 ± 18[d]	0.42 (5-H), 0.41 (2-H)
$(\mathbf{1b})_2$·KTTKS	200 ± 24[d]	2.62 (5-H), 0.39 (2-H)
1b·Ts Arg OMe	556 ± 40[d]	3.90 (5-H), 3.29, 4.09 (4-H)[b], 1.00 (2-H)
1b·RGD	653 ± 5[d]	3.41 (5-H), 0.92 (4-H), 1.50 (3-H)
1c·Ac Lys OMe	12 ± 11	3.75 (6-H), 4.41 (5-H), 2.64 (4-H), 1.29 (3-H), 0.37 (2-H)
1c·Ac Arg OMe	88 ± 5	3.86 (5-H), 2.51 (4-H), 1.32 (3-H), 0.42 (2-H)
1d·Ac Lys OMe	1164 ± 11	0.94 (6-H), 0.54 (5-H), 0.40 (4-H), 0.77, 0.52 (3-H)[b]
1d·Ac Arg OMe	1393 ± 18	0.96 (5-H), 0.62, 0.48 (4-H)[b], 0.52 (3-H)

[a]Values were determined by ^{1}H NMR titration experiments at pH = 7.2 in aqueous phosphate buffer, 75 mM for **1a**, 25 mM for **1b**, and 10 mM for **1a**·Ac Arg OMe, **1c**, and **1d**. [b]The diastereotopic methylene protons show two separate signals in the complex. [c]The signal broadening does not allow the exact ^{1}H NMR chemical shift determination of the complex. [d]Reference 9.

Chemshell v3.2 code.[23,24,26−31] The distances between the opposite C atoms of the tweezers' terminal benzene rings (Figure 4, C_p–C_p' and C_m–C_m') provide a measure of how open the tweezers are. The X–Y distance between the tweezers'

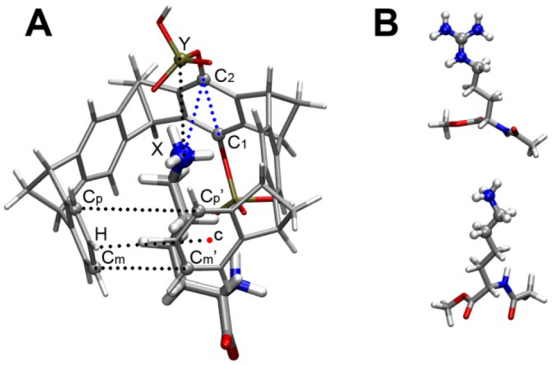

Figure 4. (A) Distances (black dotted lines) and angle (blue dotted line) used to describe the interaction between the molecular tweezers and the amino acid and peptides models (Y = P, S, or C atom of the $OCH_2CO_2^-$ group of the tweezers, X = the N atom or the central C atom of the guanidinium moiety in the lateral chain of Lys or Arg, respectively). (B) Atoms of the lateral chains of Arg and Lys included in the QM region used for the QM/MM optimizations are highlighted with a sphere representation.

X atom (X = P, S, C) and the Y atom of the guest side chain and the C_1–C_2–X angle between the opposite C atoms of the tweezers' central hydroquinone bridges and the X atom of the guest side chain illustrate the degree of insertion of the amino acid/peptide inside the tweezers' cavity (Figure 4 and Supporting Information, Table S1). The predicted C_p–C_p' and C_m–C_m' values for the isolated tweezers evidence a small dependence on the nature of the substituent. For tweezers **1a′**, **1a″**, **1c′**, and **1d′**, which have negatively charged substituents (not prone to interact with the cavity of the tweezers) the distances C_p–C_p' and C_m–C_m' are very similar (at the QM/MM level the C_p–C_p' and C_m–C_m' distances of these tweezers have values of 5.24–5.49 Å and 3.51–3.89 Å, respectively; Table S1, Supporting Information). In **1b′** the methyl group of the substituent is prone to interact with the tweezers' cavity (Figure 5). This is reflected in the larger distances for C_p–C_p' (5.94 Å) and C_m–C_m' (4.33 Å) that correspond to a more open conformation of **1b′**. For the noninteracting tweezers, the QM/MM distances are generally shorter than the MD average and the QM/MM optimized structures are less symmetric (Figure 5). This is related to the tendency of the hydrogen atoms at the end of the tweezers to interact with the π system of the aromatic ring at the opposite end side (see π-H-c distances in Figure 4 and Supporting Information, Table S1). Such behavior is best described by the QM/MM calculations in which the tweezers are treated at the quantum level with empirical dispersion corrections (B3LYP-D2).

Due to the interaction of the amino acids/peptide models with the tweezers, the C_p–C_p' and C_m–C_m' distances get somewhat shorter, indicating less open conformations of the tweezers. This is expected due to the positive charge of the side chain of Lys and Arg and the negative electronic density in the tweezers cavity. In addition, the nature of the terminal groups attached to Lys or Arg and the substituents in the tweezers also affect the tweezers structure. In the host–guest complex **1b′**·Ac Lys OMe′ the simultaneous interaction of the positive charge at the ammonium group of the Lys side chain with the anionic tweezer substituent results in an unfavorable conformation of

dx.doi.org/10.1021/jo4009673 | J. Org. Chem. 2013, 78, 6721−6734

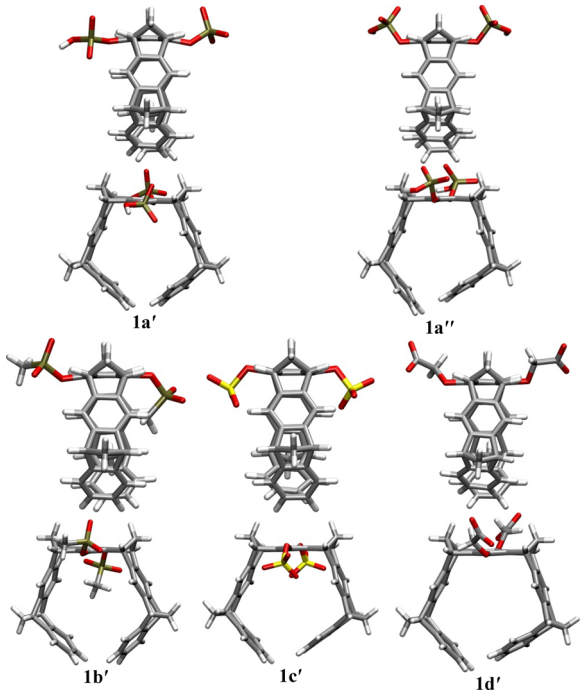

Figure 5. Structures of molecular tweezers **1a′** (≡ **1**: $R^1 = OPO_3^{2-}$, $R^2 = OP(OH)O_2^-$), **1a″** (≡ **1**: $R^1 = R^2 = OP(OH)O_2^-$), **1b′** (≡ **1**: $R^1 = R^2 = OP(Me)O_2^-$), **1c′** (≡ **1**: $R^1 = R^2 = OSO_3^-$), or **1d′** (≡ **1**: $R^1 = R^2 = OCH_2CO_2^-$) optimized by QM/MM calculations.

the lateral chain of Lys that causes the tweezer to adopt a more open conformation ($C_p-C_{p'}$ distance is 7.83 Å and $C_m-C_{m'}$ distance is 6.82 Å, QM/MM values, Table S1). The host–guest orientation in **1b′**·Ac Lys OMe′ and **1c′**·Ac Lys OMe′ is indicated by the X–Y distance and the angle C_1-C_2-X (4.06, 4.06 Å and 65°, 62° respectively, Table S1). However, the side chain in **1c′**·Ac Lys OMe′ is better oriented, and the tweezer effectively traps the amino acid side chain. The effect of the terminal group is further illustrated in **1a′**·KAA′, **1a′**·Ac Lys OMe′, and **1a′**·Ac Arg OMe′. For these systems the Lys or Arg side chain is very much threaded through the tweezer cavity with the Lys ammonium or Arg guanidinium group pointing toward the most negatively charged phosphate group of the tweezer as indicated by the value of C_1-C_2-X (89°, 98°, and 89°, respectively, Table S1). This results in some repulsion between the amino acid terminal groups and the tweezers hydrophobic body so the tweezers adopt more open conformations. For **1a′**·H Lys OH the value of C_1-C_2-X is 88°, but due to the small size of the substituent, no widening of the tweezer is observed (Table S1).

Using the QM/MM optimized structures (with an explicit, static 4-Å water layer around both the host–guest complex and the pure guest molecule as well), the ^{1}H NMR isotropic shielding constants of the guest protons in the host–guest complexes, δ_C, and in the pure guest molecules, δ_0, were computed using *ab initio* methods. The computed results are compared with the experimental values in Table 4. The full NMR shielding tensors were calculated for all nuclei within both molecular entities with the HF method using the SVP basis set,[32] employing a local development version of the Q-Chem quantum chemical software package[33] to yield the complexation-induced chemical shifts $\Delta\delta_{max}$. The reliability of the HF/SVP approach utilizing gauge including atomic orbitals (GIAO)[35−37] has been shown elsewhere for comparable systems.[17,38−40] For the calculation of the nuclear shieldings, we apply linear-scaling methods,[41,42] together with the recently

Table 4. Comparison of Experimental and Computational (HF/SVP) Complexation-Induced Chemical Shifts $\Delta\delta_{max}$ (ppm) for Guest Protons in the Host–Guest Complexes of Tweezers 1a, 1b, 1c, and 1d with Lysine and Arginine Derivatives (Table 3)[a]

host–guest complex	6-H	5-H	4-H	3-H	2-H
exptl: **1a**·H Lys OH	4.51	4.47		0.76	0.24
calcd: **1a′**·H Lys OH′	6.04	4.11	1.99	0.38	0.37
exptl: **1a**·Ac Lys OMe	3.91				0.51[b]
calcd: **1a′**·Ac Lys OMe′	3.62	5.51	4.62	1.24	2.20[b]
exptl: **1a**·KAA	5.92	3.22	2.28	1.09	0.20[c]
calcd: **1a′**·KAA′	5.71	5.08	2.55	0.36	0.06[c]
exptl: **1b**·Ac Lys OMe	>4	1.57, 1.45[d]			0.57
calcd: **1b′**·Ac Lys OMe′	3.46	3.42, 3.21[d]	1.72	0.39	2.30
exptl: **1c**·Ac Lys OMe	3.75	4.41	2.64	1.29	0.37
calcd: **1c′**·Ac Lys OMe′	4.39	3.19	1.10	0.33	0.27
exptl: **1d**·Ac Lys OMe	0.94	0.54	0.40	0.77, 0.52[d]	
calcd: (**1d′**·Ac Lys OMe′)$_{in}$	5.44	3.05	1.69	0.18, −0.92	1.33
calcd: (**1d′**·Ac Lys OMe′)$_{out}$	0.03	0.72	0.41	0.85, 0.08	0.46
exptl: **1a**·Ac Arg OMe		3.75	2.54	1.23	0.63
calcd: **1a′**·Ac Arg OMe′		5.46	2.46	0.56	1.07
exptl: **1b**·Ts Arg OMe		3.90	4.09, 3.29[d]		1.00
calcd: **1b′**·Ts Arg OMe′		4.30	2.51, 1.67[d]	0.87	−0.50
exptl: **1c**·Ac Arg OMe		3.86	2.51	1.32	0.42
calcd: **1c′**·Ac Arg OMe′		3.86	0.63	0.41	0.42
exptl: **1d**·Ac Arg OMe		0.96	0.62, 0.48[d]	0.52	
calcd: (**1d′**·Ac Arg OMe′)$_{in}$		3.36	1.39, 1.04[d]	−0.20	1.93
calcd: (**1d′**·Ac Arg OMe′)$_{out}$		0.26	0.38, 0.36[d]	0.31	0.67

[a]The *ab initio* data were calculated for the complex structures of **1a′**, **1b′**, **1c′**, and **1d′** with the corresponding lysine and arginine derivatives shown in Figure 6. [b]$\Delta\delta_{max}$: −0.32 (exptl), −0.28 (calcd), $NCOCH_3$; −0.23 (exp), −0.16 (calcd), CO_2CH_3. [c]6-, 5-, 4-, 3- ,2-H ≡ 9-, 8-, 7-, 6-, 5-H in KAA. [d]Diastereotopic H atoms.

dx.doi.org/10.1021/jo4009673 | J. Org. Chem. 2013, 78, 6721−6734

developed density matrix-based Laplace reformulation of coupled self-consistent field equations (DL-CPSCF)[42,43] In cases where the flexibility of two or more close-by rotating hydrogens yields only one peak in the experimental NMR spectrum, the calculated results were averaged accordingly over these hydrogen shifts. For diastereotopic hydrogens in host–guest species **1b**·Ac Lys OMe and **1b**·Ts Arg OMe labeled with footnote "d" in Table 4, the computed hydrogen shifts are assigned in two different possible ways and the values closer to the experimental ones are chosen to represent the calculated diastereotopic NMR shifts. This simple scheme was chosen, since there was no clear evidence that either of the diastereotopic hydrogens would favor a certain position in the optimized host–guest and pure guest structures, for example, close to the tweezers' bridge or near the tweezers' tips. The final complexation-induced NMR chemical shifts, as depicted in Table 4, were calculated as differences between the shieldings of specific nuclei in these structures. Representative calculations of complexation-induced NMR shifts for the host–guest complexes **1a**′·H Lys OH′, **1a**′·Ac Lys OMe′, and **1a**′·KAA′ with a 6-Å water layer show a maximum absolute deviation of roughly 0.4 ppm from the 4-Å results presented in Table 4.

While some of the complexation-induced shifts listed in Table 4 agree reasonably well with the experimental ^{1}H NMR chemical shifts, the mean absolute deviations (MAD) from the experimental values range from 0.6 to 1.5 ppm depending on the host–guest case (the carboxylate tweezer complexes are not considered here). Here, one should note that the complex-induced shifts range up to 6 ppm. The general trend is that the influence of the complexation on the chemical shifts increases as a function of a hydrogen position more deeply located in the host cavity. Thus, in general, the part of the guest molecule more inside the host cavity provides the largest $\Delta\delta_{max}$, and the parts furthest away from the cavity the smallest.

It should be noted that for guest molecules interacting with the carboxylate tweezer **1d**, there are two sets of different conformers. Both of these host–guest complexes were optimized by QM/MM methods and correspond to different regions in the conformational space. For these conformers, two sets of complexation-induced shifts were computed. As seen in Table 4, the computed shifts are very different for structures (**1d**′·Ac Lys OMe′)$_{in}$ and (**1d**′·Ac Lys OMe′)$_{out}$ or (**1d**′·Ac Arg OMe′)$_{in}$ and (**1d**′·Ac Arg OMe′)$_{out}$. Here most likely a rapid equilibrium between the "in" and "out" conformers of these host–guest species is expected that proceeds by rapid mutual complex formation and dissociation. Therefore, the experimental NMR shift data are evidently the average between the data of the equilibrating "in" and "out" conformers. These types of equilibria are not ruled out in the more stable cases either, although they appear to be most unlikely due to the large $\Delta\delta_{max}$ values and the better correspondence between computed and experimental data. The situation here is thus rather different from the previously studied molecular tweezers,[17,38−40] where the guest molecules were more rigid and did not have the same conformational freedom as the flexible lysine or arginine side chains. Thus, dynamical equilibria play a more important role for the present systems.

The basis set was confirmed to be adequate by carrying out HF/def2-TZVP[45] calculations, which yielded only minute changes in the $\Delta\delta_{max}$ values, and electron correlation effects, as studied with second-order Møller–Plesset perturbation theory (MP2), also play a minor role based on previous studies on similar systems.[37] Therefore, the remaining deviations between experimental and calculated chemical shifts are thus most likely attributed to the present static treatment of both the solvent-including host–guest structures and free guests. A snapshot type of averaging of NMR chemical shifts could provide a closer agreement with the experimental NMR chemical shifts, as seen for example in refs 46–50, but would require a substantial computational effort for the complex systems of the present work.

The large theoretical shifts of ^{1}H NMR guest signals, $\Delta\delta_{max}$, calculated for the methylene protons 6-H or 5-H (adjacent to the ammonium or guanidinium moiety of the lysine or arginine side chain) in the host–guest complexes with the tweezers **1a**′, **1b**′, and **1c**′ agree well (within the limit of roughly 0.5 ppm) with the experimental values ($\Delta\delta_{max}$ = 3.9 − 5.9 ppm) determined for the corresponding complexes of the tweezers **1a**, **1b**, and **1c** (Table 4). Exceptions are the complexes **1a**·H Lys OH and **1a**·Ac Arg OMe, in which the differences between the theoretical and experimental $\Delta\delta_{max}$ values of these protons are larger (up to 1.5 ppm). Larger differences between the theoretical and experimental $\Delta\delta_{max}$ values were also determined for the other side chain guest protons in the complexes of **1a**, **1b**, and **1c**, but the trend of decreasing complexation-induced shifts, $\Delta\delta_{max}$, of the ^{1}H NMR signals of the guest protons 6-H > 5-H > 4-H > 3-H > 2-H of the lysine side chain and 5-H > 4-H > 3-H > 2-H of the arginine side chain, respectively, are well reproduced by the calculations. *These findings confirm the assumption that the lysine and arginine guest molecules are bound by the phosphate-, methanephosphonate-, and sulfate-substituted tweezers **1a**, **1b**, and **1c** by threading the side chains through the tweezers' cavity with the positively charged ammonium or guanidinium end group pointing toward one of the anionic groups attached to the central benzene bridge of the tweezers.* The stability and structures of these host–guest complexes are, evidently, determined by attractive ionic, CH-π, and hydrophobic interactions. The differences between the theoretical and experimental $\Delta\delta_{max}$ values indicate that due to the flexibility of the guest side chains these host–guest complexes consist of more than one structure that exist in a dynamic equilibrium so that in the NMR spectrum only averaged signals are observed resulting from the rapidly equilibrating structures. The selective broadening of the shifted guest signals observed in the ^{1}H NMR spectra of these complexes provides further evidence for such a dynamic exchange between several structures proceeding at a rate that is similar to the NMR time scale. In the case of the phosphate tweezer **1a**, $\Delta\delta_{max}$ values of several complex structures of the phosphate and the partial protonated phosphate tweezers (**1a**′, **1a**″, **1a**‴ ≡ **1**: $R^1 = R^2 = OPO_3^{2-}$, **1**: $R^1 = OPO_3^{2-}$, $R^2 = OP(OH)O_2^-$, or **1**: $R^1 = R^2 = OP(OH)O_2^-$) with several lysine and arginine guest molecules (Supporting Information Figure S7 and Table S2) were calculated to be different from those shown in Table 4, but the trend in the shifts of the side chain ^{1}H NMR signals remains the same. This finding supports the assumption that each host–guest complex consists of several structures with the guest side chain, however, threaded through the tweezers' cavity in all cases. In the host–guest complexes of the carboxylate-substituted tweezer **1d** with Ac Lys OMe or Ac Arg OMe as guest molecules, the $\Delta\delta_{max}$ values were determined to be substantially smaller (< 1 ppm; Table 4) for the corresponding lysine or arginine side chain protons indicating complex structures in which the guest side chain is positioned outside the tweezer's cavity. The comparison of the

dx.doi.org/10.1021/jo4009673 | J. Org. Chem. 2013, 78, 6721−6734

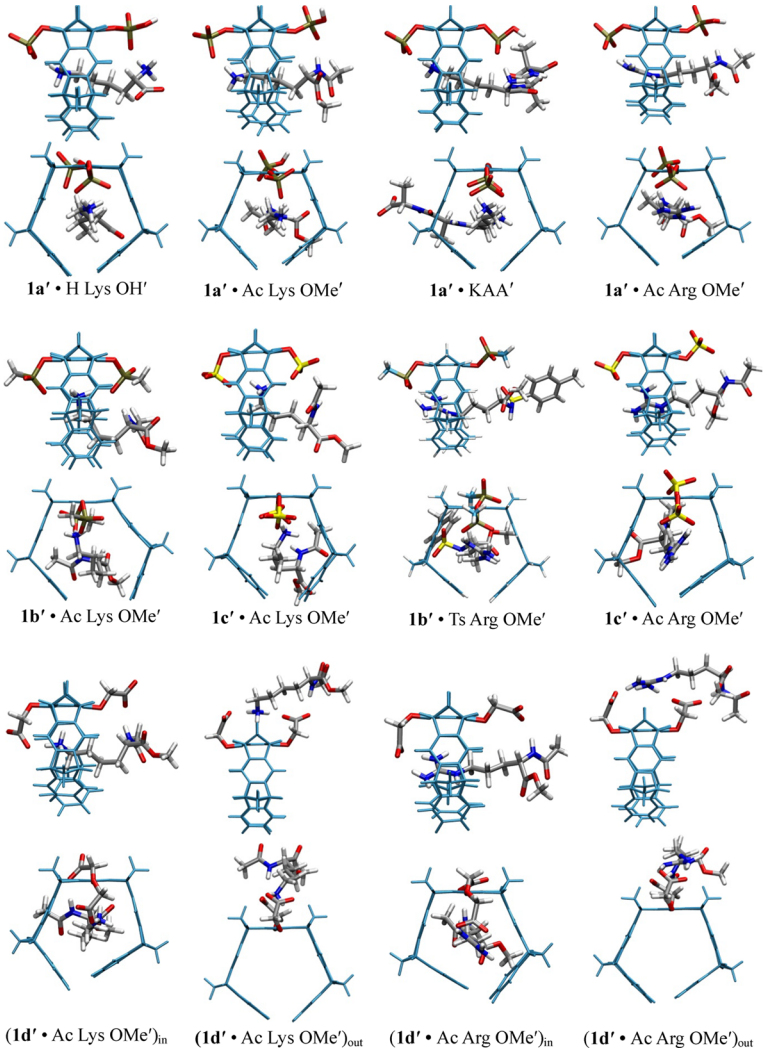

Figure 6. Two viewing angles of the host–guest complex structures of the phosphate, phosphonate, sulfate, and carboxylate tweezers **1a**′, **1b**′, **1c**′, and **1d**′ with lysine and arginine derivatives (without counterions) optimized by QM/MM calculations. Each structure contains a 60 Å water layer (not shown).

experimental $\Delta\delta_{max}$ values with theoretical values calculated for the complex structures, where the guest side chain is positioned either inside or outside the tweezer's cavity, provides good evidence that both complexes exist as rapid equilibria, (**1d**′·Ac Lys OMe′)$_{in}$ ⇌ (**1d**′·Ac Lys OMe′)$_{out}$ or (**1d**′·Ac Arg OMe′)$_{in}$ ⇌ (**1d**′·Ac Arg OMe′)$_{out}$, in each complex with preference for the outside structure. Apparently, the extended $OCH_2CO_2^-$ groups of **1d** direct the guest molecule to a position outside of the tweezer's cavitiy, and the major host–guest binding force is the electrostatic attraction between the carboxylate groups of the tweezer and the cationic ammonium or guanidinium moiety of the guest molecule. QM/MM calculations produce chelate arrangements between both carboxylates in **1d** and the complexed amino acid cation outside the tweezer's cavity; these are possible only because of the extra methylene group in the $OCH_2CO_2^-$ side chain, which is absent in **1a**, **1b**, and **1c** (Figure 6). The loss of CH-π and hydrophobic interactions in this geometry explains why the complexes of **1d** are significantly less stable than those with phosphate or sulfate tweezers **1a** or **1c**. Evidently, these host–guest binding interactions inside the tweezers' cavities of **1a–c** deliver an important contribution to the complex stability besides the ionic interaction of the tweezers' phosphate or sulfate group and the amino acid cationic side chain. A special case is methanephosphonate-substituted tweezer **1b**. The methyl group of one $OP(CH_3)O_2^-$ side chain was calculated by QM/MM to point toward the tweezer's cavity (Figure 5). Thus, the binding of a guest side chain by threading requires a rotation around the O–P bond in **1b**. This may explain why the host–guest complexes of **1b** are less stable than the corresponding complexes of **1a** and **1c**. A similar weakening of the complex stability has been observed for related host molecules bearing O-alkyl groups in the central benzene bridge in organic media. In these cases the O-alkyl groups were also calculated to point toward the host cavity and, hence, block the guest inclusion.[51] Finally the different complex stabilities of the phosphate and sulfate tweezers **1a** and **1c** certainly result from the larger negative charge of the phosphate compared to the sulfate.

Solvent Dependence of the Host–Guest Complex Formation. The solvent dependence of the amino acid binding to the tweezers is remarkable, because not only is the complex stability solvent-dependent but also the complex structure. For example, the very small complexation-induced ^{1}H NMR shifts ($\Delta\delta_{obs}$) observed for the binding of Ac Lys OMe by the phosphate tweezer **1a** in methanol (Table 5) indicate a

dx.doi.org/10.1021/jo4009673 | J. Org. Chem. 2013, 78, 6721–6734

Table 5. Solvent Dependence of Change in Intensities of the Tweezers' Emission Bands (ΔI_{max} [%] = $100(I_0 - I_{max})/I_0$, of K_d Values (Resulting from Fluorometric Titration Experiments), and of the Complexation-Induced ^{1}H NMR Shifts of the Guest Protons $\Delta\delta_{obs}$ at Host and Guest Concentration $[H]_0 = [G]_0 = 1.0$ mM[a]

					$\Delta\delta_{obs}$		
host	guest	solvent	ΔI_{max} [%]	K_d [μM]	6-H	5-H	4-H
1a	Ac Lys OMe	MeOH	−6	66 ± 11	0.24	0.28	0.26
		MeOH/PB (1:2)		nd	2.80	2.30	0.74
		PB	40	9 ± 6	3.60	3.40	1.60
	Ac Arg OMe	MeOH	0			0.76	0.44
		MeOH:PB (2:1)	0			0.72	0.46
		MeOH:PB (1:2)	nd	nd		1.45	0.96
		MeOH:PB (1:9)	27	157 ± 8		2.16	1.47
		PB	47	20 ± 5		3.30	2.19
1c	Ac Lys OMe	MeOH	−44	20 ± 6	2.96	3.25	1.75
		PB	44	19 ± 3	3.40	3.30	1.30
	Ac Arg OMe	MeOH	−22	276 ± 7		0.67	0.30
		PB	30	77 ± 5		2.67	1.70
1d	Ac Lys OMe	PB	36	643 ± 7	0.94[b]	0.54[b]	0.40[b]
	Ac Arg OMe	PB	13	281 ± 18		0.96[b]	0.62[b]

[a] I_0 = emission intensity of free tweezers, I_{max} = emission intensity of host-guest complexes. The standard deviation of K_d is given in %. PB = aqueous phosphate buffer (10 mM) at pH = 7.2; nd = not determined. [b] $\Delta\delta_{max}$.

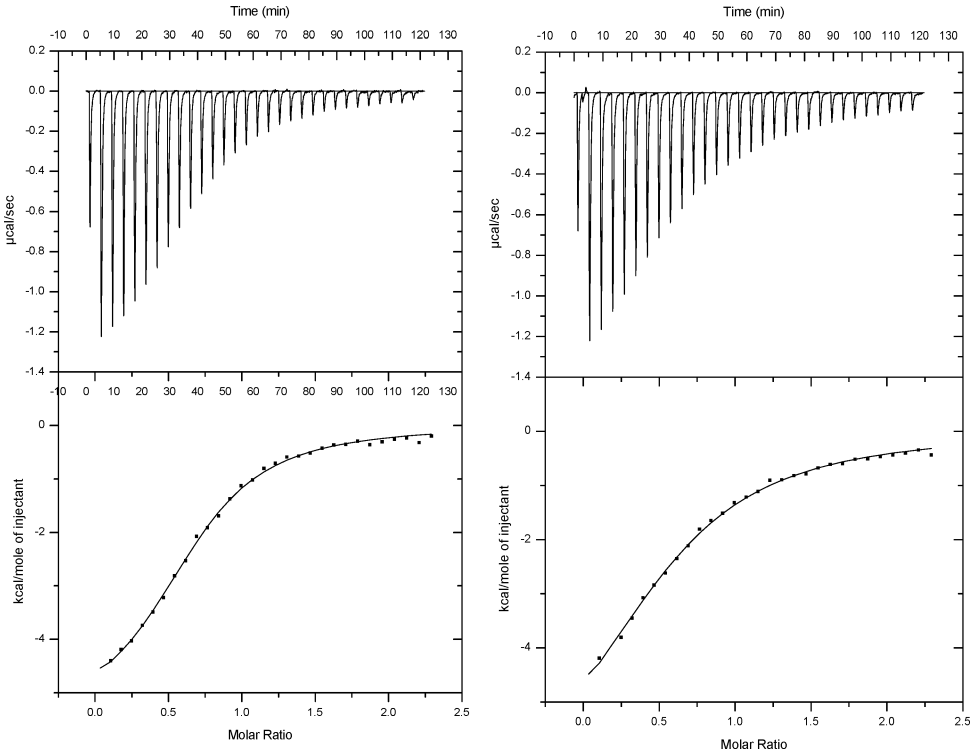

Figure 7. Plots of the isothermal titration calorimetry (ITC) measurements in aqueous phosphate buffer (10 mM, pH = 7.6) for the complex formation between phosphate tweezer **1a** and Ac Lys OMe (left) and **1a** and Ac Arg OMe (right).

complex structure where the guest molecule is positioned outside the tweezer cavity comparable to the host−guest complex structures of the carboxylate tweezer **1d** discussed in the previous paragraph. Evidently, the ionic interaction between one of the negatively charged host phosphate groups and the positively charged guest ammonium group is the dominating binding force in methanol and the weakened contribution of dispersive and hydrophobic interactions gained by amino acid side chain threading seems to be less important in methanol.[52]

At the same time, the intensity of the tweezer's emission band is increased on guest binding in methanol but quenched in aqueous buffer (**1a**·Ac Lys OMe). We conclude that the direction and extent of emission intensity change also provides structural information. In the mixture of methanol with aqueous phosphate buffer (1:2) containing **1a** and Ac Lys OMe, relatively large $\Delta\delta_{obs}$ values were observed (Table 5) indicating that the complex is at least partially formed by threading of the lysine side chain into the tweezer's cavity comparable to the complex formation in pure aqueous phosphate buffer. In this solvent mixture, however, no change in the tweezer's emission intensity could be detected by the addition of Ac Lys OMe. These findings strongly suggest that

dx.doi.org/10.1021/jo4009673 | J. Org. Chem. 2013, 78, 6721−6734

Table 6. Thermodynamic Parameters for Complex Formation between Molecular Tweezers 1a or 1c and Lysine- or Argine-Containing Guest Molecules[a]

host	guest	K_a	ΔG	ΔH	$-T\Delta S$	K_d
1a	Ac Lys OMe	6.86 ± 0.07	−6.6 ± 0.1	−5.6 ± 0.1	−1.0 ± 0.1	14.6 ± 0.2
1a	Ac Arg OMe	2.96 ± 0.21	−6.1 ± 0.1	−7.0 ± 0.2	+0.9 ± 0.3	34.0 ± 0.3
1a	KLVFF	6.56 ± 0.26	−6.6 ± 0.1	−6.4 ± 0.1	−0.2 ± 0.1	15.2 ± 0.1
1c	Ac Lys OMe	3.46 ± 0.16	−6.2 ± 0.1	−8.3 ± 0.1	+2.1 ± 0.1	28.9 ± 1.3
1c	Ac Arg OMe	1.04 ± 0.09	−5.5 ± 0.1	−6.3 ± 0.4	+0.8 ± 0.5	96.9 ± 8.4

[a]Parameters include binding constant K_a [10^4 M^{-1}], binding Gibbs enthalpy ΔG [kcal/mol], binding enthalpy ΔH [kcal/mol], binding entropy $T\Delta S$ [kcal/mol], and dissociation constant K_d [μM] (= $1/K_a$).Values were determined by isothermal titration calorimetry (ITC) measurements in aqueous phosphate buffer (10 mM, pH = 7.6). In each case, the listed values are the average of two independent measurements, and the listed errors are the deviations from the mean values of the two measurements.

the fluorescence is quenched if the guest is bound inside the tweezer's cavity and increased if the guest is bound outside the cavity. In certain mixtures of methanol and aqueous buffer these two effects seem to compensate each other, so that no intensity change of the tweezer's emission band occurs on the addition of the guest molecule.

Determination of the Thermodynamic Parameters of the Host–Guest Complex Formation by Isothermal Titration Calorimetry (ITC). The thermodynamic parameters for the host–guest complex formation of the phosphate- and sulfate-substituted tweezers **1a** and **1c** with several lysine and arginine guest molecules were also determined by isothermal titration calorimetry (ITC). Figure 7 shows the plots of titration for the binding of Ac Lys OMe and Ac Arg OMe by tweezer **1a** as representative examples. The dissociation constants (K_d, Table 6) agree well with the data determined independently by fluorometric or ^{1}H NMR titration experiments (Table 2 and 3). The additional thermodynamic parameter, the binding enthalpy ΔH and entropy $T\Delta S$, obtained by the ITC measurements, provide further insight into the binding mode. The more negative ΔH value determined for the formation of **1a**·Ac Arg OMe indicates that the arginine guest is enthalpically bound tighter to **1a** than the corresponding lysine guest. This tighter enthalpic binding of Ac Arg OMe is overcompensated by a less favorable entropy so that the complex **1a**·Ac Lys OMe is more stable (has a smaller dissociation constant, K_d) than **1a**·Ac Arg OMe. This kind of enthalpy–entropy compensation is often found in supramolecular systems.[53] Here the arginine guest loses degrees of rotational freedom inside the tweezer cavity due to its rigid delocalized guanidinium ion, as opposed to lysine's small localized ammonium ion that continues to rotate around its C–N and C–C bonds inside the tweezer cavity. In addition, the localized lysine ammonium cation is certainly solvated by more water molecules than the delocalized arginine guanidinium cation so that in the former case more water molecules are released to the bulk than in the case of arginine; this is also entropically favorable. Similar results were earlier obtained for the complex formation of a sulfonatocalix[4]arene derivative with lysine or arginine in water.[3b] Also in this case, lysine binding to the calixarene was entropically favored whereas arginine complexation produced the larger enthalpy gain. Transition to host–guest complex formation between the sulfate-substituted tweezer **1c** and Ac Lys OMe or Ac Arg OMe furnishes K_d values determined by ITC that again agree well with those determined by fluorescence or ^{1}H NMR titration experiments. In these cases, however, both enthalpy and entropy changes are more negative for Ac Lys OMe complexation than those measured for Ac Arg OMe. There is no obvious explanation for these differences between **1a** and **1c**. Assistance comes from close inspection of the calculated complex structures (Figure 6): the guanidinium cation of the arginine side chain is more tightly bound to the doubly charged phosphate anion from **1a** than to the singly charged sulfate anion from **1c**, which coincides with the superior enthalpy gain of the phosphate tweezer. On the other hand, the calculated structure of **1c**·Ac Lys OMe suggests a chelate-type interaction between lysine's ammonium inside the tweezer's cavity and both sulfate arms from **1c** - which leads to a powerful enthalpy gain at the cost of a substantial entropy loss.

CONCLUSION

The behavior of the water-soluble molecular tweezers **1a–d** (bearing phosphate, methanephosphonate, sulfate, or OCH_2-carboxylate groups in their central benzene bridge) was investigated in buffered aqueous solution at almost neutral pH by three independent methods (fluoroscence, NMR, and ITC titration experiments). They all form stable host–guest complexes with various amino acid and peptide guests containing either lysine or arginine moieties. In the case of tweezers **1a–c** large complexation-induced shifts of the ^{1}H NMR guest signals ($\Delta\delta_{max} \leq 6$ ppm) were found for the methylene protons of the lysine or arginine side chain. These agree well with theoretical data calculated by a combination of QM/MM and *ab initio* methods for the host–guest complex structures shown in Figure 6. This correlation provides experimental evidence for the postulated binding mode: the lysine or arginine side chain is literally threaded through the tweezers' cavity with its positively charged ammonium or guanidinium end group pointing toward one of the anionic groups on the tweezers' central benzene bridge. Thus, attractive ionic, CH-π, and hydrophobic interactions are the major binding forces that determine the stability and structures of these host–guest complexes. Substantially smaller complexation-induced shifts of the corresponding ^{1}H NMR guest signals ($\Delta\delta_{max} < 1$ ppm) were found for the host–guest complexes of the carboxylate-substituted tweezer **1d** with Ac Lys OMe or Ac Arg OMe as guest molecule. Comparison of experimental with theoretical $\Delta\delta_{max}$ values calculated for the complex structures with included or externally bound guest (Figure 6) indicates that both complexes exist as rapid equilibria, (**1d′**·Ac Lys OMe′)$_{in}$ ⇌ (**1d′**·Ac Lys OMe′)$_{out}$ or **1d′**·Ac Arg OMe′)$_{in}$ ⇌ (**1d′**·Ac Arg OMe′)$_{out}$, in each complex with a significant preference for the external binding mode. The extended $OCH_2CO_2^-$ groups of **1d** appear to direct the guest side chain to an external position (outside of the tweezer's cavity), and the major binding force becomes the electrostatic attraction between the tweezer carboxylates and the amino acid

dx.doi.org/10.1021/jo4009673 | J. Org. Chem. 2013, 78, 6721–6734

ammonium or guanidinium moiety. The loss of CH-π and hydrophobic interactions explains why these complexes are significantly less stable than those with phosphate or sulfate tweezers **1a** or **1c**. QM/MM calculations produce chelate arrangements between both carboxylates in **1d** and the complexed amino acid cation; these are preferred for **1d** complexes because of the extra methylene group, which is absent in **1a** and **1c**. Solvent-dependence and ITC measurements provide further insight into the noncovalent host−guest binding modes. In methanol ionic interactions between amino acid cation and tweezers anions become the dominating binding force for all tweezers. Now, the guest side chain is preferentially positioned outside each tweezers' cavity; this is most likely caused by the absence of the hydrophobic effect in this solvent; in addition, methanol molecules may occupy the cavity. As a consequence, the hydrophobic effect in water seems to be the major force that drags the guest molecule into the cavity of the tweezers. The thermodynamic parameters (enthalpy, ΔH, and entropy, $T\Delta S$) determined by ITC (Table 6) indicate powerful enthalpy-driven guest attraction, featuring an enthalpy−entropy compensation that is often observed in supramolecular systems.[53] In complex **1a**·Ac Arg OMe a stronger enthalpic host−guest binding ($\Delta H_{(\mathbf{1a}\cdot\text{Ac Arg OMe})} < \Delta H_{(\mathbf{1a}\cdot\text{Ac Lys OMe})}$) is overcompensated by an unfavorable more negative entropic parameter ($T\Delta S_{(\mathbf{1a}\cdot\text{Ac Arg OMe})} < T\Delta S_{(\mathbf{1a}\cdot\text{Ac Lys OMe})}$) compared to **1a**·Ac Lys OMe, so that the later complex is more stable at room temperature. The thermodynamic parameters of the corresponding complexes of the sulfate tweezer **1c** show no similar enthalpy−entropy compensation. This different behavior of complexes of **1c** can be explained by inspection of the calculated complex structures (Figure 6). In the structure of **1c**′·Ac Lys OMe′ the guest ammonium group is calculated to interact with both tweezer sulfate groups, leading to a restriction of the rotation of guest side chain inside the tweezer cavity, which may explain the negative entropy parameter compared to **1a**·Ac Lys OMe. The experimentally observed properties of the tweezers **1a**, **1b**, and **1c** on one side and **1d** on the other side are in good accord with the calculation by means of molecular mechanics and quantum chemical methods. These findings provide good confidence into the methods applied here for the elucidation of the host−guest structures and stabilities.Thus, the combination of experiment and theory provide deep insight into the binding modes of these molecular tweezers to the amino acids lysine and arginine, which is an essential prerequisite for the understanding of the intriguing effect of these tweezers on the aggreation of proteins and the activity of enzymes.

EXPERIMENTAL SECTION

General Experimental Details. ^{1}H NMR, ^{13}C NMR, DEPT H,H−COSY, C,H−COSY, NOESY, HMQC, and HMBC titration experiments were carried out by using a 500 MHz spectrometer. The undeuterated amount of the solvent was used as an internal standard. The ^{1}H and ^{13}C NMR signals were assigned by the 2D experiments mentioned above. Positions of the protons of the methano bridges are indicated by the letters *i* (*innen*, toward the center of the molecule) and *a* (*aussen*, away from the center of the molecule). The numbering of the atoms in the tweezers is shown in the Supporting Information. Fluorescence spectra were measured on a spectrofluorometer. Mass spectra were recorded on an ESI-TOF mass spectrometer. Isothermal titration calorimetry (ITC) measurements were carried out by the use of a microcalorimeter at 25.0 °C. All melting points (mp) are uncorrected. All solvents were distilled prior to use.

Sulfate Tweezer 1c. A stirred solution of 75 mg (0.132 mmol) of the dihydroxy tweezer **1e** and 85 mg (0.53 mmol) of sulfur trioxide pyridinium complex in 7 mL of dry pyridine was heated under reflux at 90 °C for 24 h. Then, an additional 63 mg (0.397 mmol) of SO_3·Py complex was added to this solution, and the mixture was stirred for another 36 h at the same temperature. The mixture was cooled to rt and quenched with saturated aqueous $NaHCO_3$ solution. The excess of inorganic salts was filtered off by a glass filter (D4), and the aqueous filtrate was extracted with diethyl ether (3 × 50 mL). The solvent of the aqueous phase was distilled off in vacuum in a rotary evaporator. The solid residue was suspended in ethanol and filtered off. The solvent of the filtrate was removed in a rotary evaporator, and the remaining solid was dried in oil pump vacuum. The tweezer **1c** was collected as white solid. Yield: 70 mg, 68%; mp >229 °C (decomposition). ^{1}H NMR (500 MHz, CD_3OD): δ [ppm] 2.26 (td, 2H, H-24a, H-25a), 2.33 (s, 4H, H-23, H-26), 2.51 (td, 2H, H-24i, H-25i), 4.00 (4H, H-5, H-11, H-16, H-22), 4.48 (s, 4H, H-7, H-9, H-18, H-20), 6.78 (m, 4H, 4H, H-2, H-3, H-13, H-14), 7.02 (m, 4H, H-4, H-12, H-1, H-15), 7.10 (s, 4H, H-6, H-10, H-17, H-21). ^{1}H NMR (500 MHz,D_2O): δ [ppm] 2.34 (d, 2H, H-24a, H-25a), 2.39 (m, 4H, H-23, H-26), 2.48 (d, 2H, H-24i, H-25i), 4.20 (4H, H-5, H-11, H-16, H-22), 4.45 (s, 4H, H-7, H-9, H-18, H-20), 6.06 (br, s, 4H, 4H, H-2, H-3, H-13, H-14), 7.03 (m, 4H, H-4, H-12, H-1, H-15), 7.18 (s, 4H, H-6, H-10, H-17, H-21). ^{13}C NMR (125,7 MHz, CD_3OD): δ [ppm] 50.0 (C-7, C-9, C-18, C-20), 52.4 (C-5, C-11, C-16, C-22), 69.0, 69.4 (C-23, C-24, C-25, C-26), 117.3 (C-6, C-10, C-17, C-21), 122.1 (C-4, C-12, C-1, C-15), 125.8 (C-2, C-3, C13, C-14), 139.3 (C-8, C-19) 144.8 (C-7a, C-8a, C-18a, C-19a), 148.6 (C-6a, C-9a, C-17a, C-20a), 149.2 (C-5a, C-10a, C-16a, C-21a), 151.9 (C-4a, C-11a, C-15a, C-22a). HRMS (ESI-TOF) *m*/*z*: $[M + Na]^+$ calcd for $C_{42}H_{28}O_8S_2Na_3$ 793.0913, found 793.0944; *m*/*z* $[M - Na]^-$ calcd for $C_{42}H_{28}O_8S_2Na$ 747.1129, found 747.1131; *m*/*z* $[M - 2Na]^{2-}$ calcd for $C_{42}H_{28}O_8S_2$ 362.0618, found 362.0635.

Methyl Carboxylate Tweezer 1g. Under argon atmosphere 20 mg (0.035 mmol) of the dihydroxy tweezer **1e** was dissolved in 20 mL of dry acetone. Then 21.5 mg (0.14 mmol, 0.013 mL) of methyl bromoacetate, 19 mg of potassium carbonate (0.14 mmol), and a few granules of potassium iodide were added to this solution, and the mixture was stirred for 4 days at room temperature. Dichloromethane (50 mL) was added to this mixture, and the solution was washed with saturated aqueous NH_4Cl, saturated aqueous $NaHCO_3$, and distilled water. The organic phase was dried over Na_2SO_4, and the solvent was removed in vacuum in a rotary evaporator. The oily residue was purified by column chromatography (silica gel, cyclohexane/EtOAc 3:1) leading to tweezer **1g** substituted by OCH_2CO_2Me groups as colorless solid. Yield: 25 mg of **1g** (0.030 mmol, 99%); mp 240 °C (decomposition). ^{1}H NMR (500 MHz,$CDCl_3$): δ [ppm] 2.35 (m, 4H, H-23, H-26), 2.43 (m, 4H, H-24, H-25), 3.66 (s, 6H, H-29, H-30), 4.08 (m, 4H, H-5, H-11, H-16, H-22), 4.27 (m, 4H, H-7, H-9, H-18, H-20), 4.38 (s, 4H, H-27, H-28), 6.76 (m, 4H, H-2, H-3, H-13, H-14), 7.08 (m, 4H, H-1, H-4, H-12, H-15), 7.14 (s, 4H, H-6, H-10, H-17, H-21). ^{13}C NMR(125 MHz,$CDCl_3$): δ [ppm] 14.4 (C-29, C-30), 48.5 (C-7, C-9, C-18, C-20), 51.5 (C-5, C-11, C-16, C-22), 69.3 (C-24, C-25), 69.9 (C-23, C-26), 70.7 (C-27, C-28), 116.4 (C-6, C-10, C-17, C-21), 121.6 (C-1, C-4, C-12, C-15), 124.7 (C-2, C-3, C-13, C-14), 140.3 (C-7a, C-8a,C-18a, C-19a), 144.5 (C-8, C-19), 147.1 (C-6a, C-9a, C-17a, C-20a), 147.8 (C-5a, C-10a, C-16a, C-21a), 150.6 (C-4a, C-11a, C-15a, C-22a), 170.1 (C-27a, C-28a). HRMS (ESI-TOF): *m*/*z* $[M + Na^+]$ calcd for $C_{48}H_{38}O_6Na$ 733.2561, found 733.2567.

Carboxylate Tweezer 1d. NaOH·H_2O (0.082 mmol) was added to the stirred solution of 29 mg (0.041 mmol) of methyl carboxylate tweezer **1g** in 5 mL of dry methanol. After 1 h of stirring the solvent was removed in a rotary evaporator, and the solid residue was dried in vacuum. Yield of **1d**: 30 mg (0.041 mmol, >99%); mp > 255 °C (decomposition). ^{1}H NMR (500 MHz, D_2O): δ [ppm] 2.36 (m, 8H, H-23, H-24, H-25, H-26), 4.03 (s, 4H, H-5, H-11, H-16, H-22), 4.18 (s, 4H, H-7, H-9, H-18, H-20), 4.33 (s, 4H, H-27, H-28), 6.75 (br s, 4H, H-2, H-3, H-13, H-14), 7.16 (br s, 4H, H-1, H-4, H-12, H-15), 7.27 (s, 4H, H-6, H-10, H-17, H-21). ^{13}C NMR (125 MHz, D_2O): δ [ppm] 47.8 (C-7, C-9, C-18, C-20), 50.8 (C-5, C-11, C-16, C-22),

dx.doi.org/10.1021/jo4009673 | J. Org. Chem. 2013, 78, 6721−6734

68.0 (C-24, C-25), 68.3 (C-23, C-26), 72.5 (C-27, C-28), 116.2 (C-6, C-10, C-17, C-21), 121.5 (C-1, C-4, C-12, C-15), 125.2 (C-2, C-3, C-13, C-14), 141.0 (C-7a, C-8a,C-18a, C-19a), 143.6 (C-8, C-19), 147.9 (C-6a, C-9a, C-17a, C-20a), 148.5 (C-5a, C-10a, C-16a, C-21a), 151.0 (C-4a, C-11a, C-15a, C-22a), 177.0 (COO^-). HRMS (ESI- TOF): *m*/*z* $[M - 2Na^+]^{2-}$ calcd for $C_{46}H_{32}O_6$ 340.1094, found 340.1088.

Dimerization of the Molecular Tweezers Determined by ^{1}H NMR Titration. The concentration-dependent chemical shifts δ_{obs} observed in the ^{1}H NMR spectrum of the tweezers **1a** and **1c** in aqueous solution are averaged values between the monomeric (δ_0) and dimeric tweezers structure (δ_{dim}), provided that the mutual association and dissociation are fast with respect of the NMR time scale. The dimerization constants K_{dim} [M^{-1}] and the maximum complexation-induced shifts of the tweezers ^{1}H NMR signals $\Delta\delta_{max}$ [ppm] were determined from the concentration dependence of the ^{1}H NMR chemical shifts of the tweezers protons (shown in the Supporting Informatin) by using the following equation:

$$\Delta\delta = \frac{\Delta\delta_{max}}{[R]_0}\cdot\left[[R]_0 + \frac{1}{4\cdot K_{dim}} - \sqrt{\frac{[R]_0}{2\cdot K_{dim}} + \frac{1}{16\cdot K_{dim}^2}}\right]$$

Fluorescence Titrations. In a spectrofluorometer, the solution of the fluorescent tweezers was excited at a wavelength as described in the Supporting Information, and the emission spectra were monitored in the range of 300 to 600 nm. In a typical titration experiment, 700 μL of the host solution was placed in a quartz cuvette, and the guest solution was added stepwise. Emission intensity changes were recorded at 25 °C; from their concentration dependence the association constants K_a and, hence, the dissociation constants K_d ($K_d = 1/K_a$) were determined by standard nonlinear regression. Thus, the total host concentration $[H]_0$ was kept constant, whereas the total guest concentration $[G]_0$ was varied, and K_a and ΔI_{max} were calculated from the dependence of $\Delta I(=\Delta I_{obs} = I_0 - I_{obs})$ of the guest concentration by using eq 1a.

$$\Delta I = \frac{\Delta I_{max}}{[H]_0}\cdot\left(\frac{1}{2}\left([H]_0 + [G]_0 + \frac{1}{K_a}\right) - \sqrt{\frac{1}{4}\cdot\left([H]_0 + [G]_0 + \frac{1}{K_a}\right)^2 - [H]_0\cdot[G]_0}\right) \quad (1a)$$

^{1}H NMR Titrations. The association constants, K_a, and the maximum complexation-induced chemical ^{1}H NMR shifts of the guest protons, $\Delta\delta_{max}$, were determined by ^{1}H NMR titration as described in ref 39. Host H (= Receptor R) and guest G (= Substrate S) are in a fast equilibrium with the 1:1 complex HG. Thus, the observed chemical shift δ_{obs} of the guest proton in the ^{1}H NMR spectrum of a host and guest mixture is an averaged value between free (δ_0) and complexed guest (δ_{HG}). Two types of experiments were carried out to determine K_a and $\Delta\delta_{max}$: (1) The total guest concentration $[G]_0$ was kept constant, whereas the total host concentration $[H]_0$ was varied and K_a and $\Delta\delta_{max}$ were calculated from the dependence of $\Delta\delta$ ($= \Delta\delta_{obs} = \delta_0 - \delta_{obs}$) of the host concentration by using eq 1b. (2) A host and guest mixture with constant host and guest ratio was diluted, and K_a and $\Delta\delta_{max}$ were again calculated from the dependence of $\Delta\delta$ ($= \delta_0 - \delta_{obs}$) of the host concentration by using eq 2.

$$\Delta\delta = \frac{\Delta\delta_{max}}{[G]_0}\left(\frac{1}{2}\left([H]_0 + [G]_0 + \frac{1}{K_a}\right) - \sqrt{\frac{1}{4}\left([H]_0 + [G]_0 + \frac{1}{K_a}\right)^2 - [H]_0[G]_0}\right) \quad (1b)$$

$$\Delta\delta = \frac{\Delta\delta_{max}}{2}\left(K + 1 + \frac{K}{[H]_0K_a} - \sqrt{K^2 + \frac{2K^2}{[H]_0K_a} - 2K + \frac{K^2}{[H]_0^2K_a^2} + \frac{2K}{[H]_0K_a} + 1}\right) \quad (2)$$

with $K = [H]_0/[G]_0$.

■ ASSOCIATED CONTENT

Supporting Information

^{1}H NMR spectra of the new molecular tweezers **1c**, **1d**, and **1g**, dimerization of the molecular tweezers determined by ^{1}H NMR titration, host–guest complex formation of the molecular tweezers with various amino acid and peptide guest molecules containing lysine or arginine moieties determined by fluorescence titration, ^{1}H NMR titration, and ITC experiments. Computational methods: calculation of host–guest complex structures by QM/MM. Calculation of ^{1}H NMR shifts of the guest signals by *ab initio* methods. This material is available free of charge via the Internet at http://pubs.acs.org.

■ AUTHOR INFORMATION

Corresponding Author

*E-mail: esanchez@mpi-muelheim.mpg.de; christian.ochsenfeld@uni-muenchen.de; frank.klaerner@uni-duisburg-essen.de; thomas.schrader@uni-due.de.

Notes

The authors declare no competing financial interest.

■ ACKNOWLEDGMENTS

We thank Professor Paola Ceroni (Department of Chemistry, University of Bologna, Italy) for the measurement of the fluorescence spectra of molecular tweezers. E.S.-G. and K.B.-R. acknowledge Liebig and doctoral stipends from the Fonds der Chemischen Industrie, Germany. E.S.-G. acknowledges the support of the Cluster of Excellence 'Ruhr Explores Solvation' RESOLV (EXC 1069) funded by the Deutsche Forschungsgemeinschaft. M.H. and C.O. thanks Dr. Matthias Beer, Dr. Jörg Kussman. and Dr. Boris Maryasin (LMU Munich) for useful discussions. C.O. acknowledges financial support by the Volkswagen Stiftung within the funding initiative 'New Conceptual Approaches to Modeling and Simulation of Complex Systems', by the SFB 749 'Dynamik und Intermediate molekularer Transformationen' (DFG), and the DFG cluster of excellence 'Center for Integrative Protein Science Munich' (CIPSM).

■ REFERENCES

(1) Lehn, J.-M. *Supramolecular Chemistry, Concepts and Perspectives*; VCH Verlagsgesellschaft mbH: Weinheim, Germany

(2) (a) Lehn, J. M.; Vierling, P.; Hayward, R. *J. Chem. Soc., Chem. Commun.* **1979**, 296–298. (b) Hossain, M. A.; Schneider, H.-J. *J. Am. Chem. Soc.* **1998**, *120*, 11208–11209. (c) Mandl, C. P.; König, B. *J. Org. Chem.* **2005**, *70*, 670–674.

(3) (a) Douteau-Guével, N.; Coleman, A. W.; Morel, J.-P.; Morel-Desrosiers, N. *J. Phys. Org. Chem.* **1998**, *11*, 693–696. (b) Douteau-Guével, N.; Coleman, A. W.; Morel, J.-P.; Morel-Desrosiers, N. *J. Chem. Soc., Perkin Trans. 2* **1999**, 629–633. (c) Douteau-Guével, N.; Perret, F.; Coleman, A. W.; Morel, J.-P. *J. Chem. Soc., Perkin Trans. 2* **2002**, 524–532. (d) Dziemidowicz, J.; Witt, D.; Rachón, J. *J. Incl. Phenom. Macrocycl. Chem.* **2008**, *61*, 381–391. (e) Review: Mutihac, L.; Lee, J. H.; Kim, J. S.; Vicens, J. *Chem. Soc. Rev* **2011**, *40*, 2777–2796.

(4) Ngola, S. M.; Kearney, P. C.; Mecozzi, S.; Russell, K.; Dougherty, D. A. *J. Am. Chem. Soc.* **1999**, *121*, 1192−1201.
(5) Bell, T. W.; Khasanov, A. B.; Drew, M. G. B.; Filikov, A.; James, T. L. *Angew. Chem., Int. Ed.* **1999**, *38*, 2543−2547.
(6) Öberg, C. T.; Noresson, A.-L.; Leffler, H.; Nilsson, U. J. *Chem.—Eur. J.* **2011**, *17*, 8139−8144.
(7) Braxmeier, T.; Demarcus, M.; Fessmann, T.; McAteer, S.; Kilburn, J. D. *Chem.—Eur. J.* **2001**, *7*, 1889−1898.
(8) Villari, V.; Mineo, P.; Scamporrino, E.; Micali, N. *Chem. Phys.* **2012**, *402*, 118−123.
(9) Fokkens, M.; Schrader, T.; Klärner, F.-G. *J. Am. Chem. Soc.* **2005**, *127*, 14415−14421.
(10) Talbiersky, P.; Bastkowski, F.; Klärner, F.-G.; Schrader, T. *J. Am. Chem. Soc.* **2008**, *130*, 9824−9828.
(11) (a) Sinha, S.; Lopes, D. H. J.; Du, Z.; Pang, E. S.; Shanmugam, A.; Lomakin, A.; Talbiersky, P.; Tennstaedt, A.; McDaniel, K.; Bakshi, R.; Kuo, P.-Y.; Ehrmann, M.; Benedek, G.-B.; Loo, J. A.; Klärner, F.-G.; Schrader, T.; Wang, C.; Bitan, G. *J. Am. Chem. Soc.* **2011**, *133*, 16958−16969. (b) Sinha, S.; Du, Z.; Maiti, P.; Klärner, F.−G.; Schrader, T.; Wang, C.; Bitan, G. *ACS Chem. Neurosci.* **2012**, *3* (6), 451−458.
(12) Prabhudesai, S.; Sinha, S.; Attar, A.; Kotagiri, A.; Fitzmaurice, A. G.; Lakshmanan, R.; Ivanova, M. I.; Loo, J. A.; Klärner, F.-G.; Schrader, T.; Stahl, M.; Bitan, G.; Bronstein, J. M. *Neurotherapeutics* **2012**, *9*, 464−476.
(13) Review: Klärner, F.-G.; Schrader, T. *Acc. Chem. Res.* **2013**, *46*, 967−978.
(14) Bier, D.; Rose, R.; Bravo-Rodriguez, K.; Bartel, M.; Ramirez-Anguita, J. M.; Dutt, S.; Wilch, C.; Klärner, F.-G.; Sanchez-Garcia, E.; Schrader, T.; Ottmann, C. *Nat. Chem.* **2013**, *5*, 234−239.
(15) Klärner, F.-G.; Burkert, U.; Kamieth, M.; Boese, R.; Benet-Buchholz, J. *Chem.—Eur. J.* **1999**, *5*, 1700−1707.
(16) **1g** is analoguous to the known ethylester-substituted tweezer **1** (R^1 = R^2 = OCH_2CO_2Et): Klärner, F.-G.; Benkhoff, J.; Boese, R.; Burkert, U.; Kamieth, M.; Naatz, U. *Angew. Chem., Int. Ed. Engl.* **1996**, *35*, 1130−1133. The $OCH_2CO_2^-Cs^+$-substituted tweezer, which is analogous to **1d**, was prepared by Klärner, F.-G.; Burkert, U.; Kamieth, M.; Boese, R. *J. Phys. Org. Chem.* **2000**, 604−611.
(17) Klärner, F.-G.; Kahlert, B.; Nellesen, A.; Zienau, J.; Ochsenfeld, C.; Schrader, T. *J. Am. Chem. Soc.* **2006**, *128*, 4831−4841; *J. Am. Chem. Soc.* **2010**, *132*, 4029.
(18) The results of the calculation obtained for the dimer structures of the benzene-bridged tweezers **1a** and **1c** agree well with those obtained for the dimer of the related naphthalene-bridged tweezer where quantum chemical *ab initio* ^{1}H NMR shift calculations confirmed the assumed structure.[17]
(19) Review. Interaction of KAA with vancomycin: Williams, D. H.; Bardsley, B. *Angew. Chem., Int. Ed.* **1999**, *38*, 1172−1193.
(20) Tjernberg, L. O.; Lilliehook, C.; Callaway, D. J. E.; Naslund, J.; Hahne, S.; Thyberg, J.; Terenius, L.; Nordstedt, C. *J. Biol. Chem.* **1997**, *272*, 12601−12605.
(21) Guttman, C. *Dermatol. Times* **2002**, *Sept 1*.
(22) Hynes, R. O. *Cell* **1992**, *69*, 11−25.
(23) Brooks, B. R.; Bruccoleri, R. E.; Olafson, B. D.; States, D. J.; Swaminathan, S.; Karplus, M. *J. Comput. Chem.* **1983**, *4*, 187−217.
(24) Mackerell, A. D.; Feig, M.; Brooks, C. L. *J. Comput. Chem.* **2004**, *25*, 1400−1415.
(25) Jorgensen, W. L.; Chandrasekhar, J.; Madura, J. D.; Impey, R. W.; Klein, M. L. *J. Chem. Phys.* **1983**, *79*, 926−935.
(26) Zoete, V.; Cuendet, M. A.; Grosdidier, A.; Michielin, O. *J. Comput. Chem.* **2011**, *32*, 2359−2368.
(27) *Chemshell, a Computational Chemistry Shell* (www.chemshell.org).
(28) Lee, C.; Yang, W.; Parr, R. G. *Phys. Rev. B* **1988**, *37*, 785−789.
(29) Grimme, S. *J. Comput. Chem.* **2006**, *27*, 1787−1799.
(30) Schafer, A.; Horn, H.; Ahlrichs, R. *J. Chem. Phys.* **1992**, *97*, 2571−2577.
(31) Senn, H. M.; Thiel, W. *Angew. Chem. I. E.* **2009**, *48*, 1198−1229.
(32) Schäfer, A.; Horn, H.; Ahlrichs, R. *J. Chem. Phys.* **1992**, *97*, 2571−2577.
(33) *Development version of the Q-Chem program package*, 2012 (http://www.q-chem.com).
(34) London, F. *J. Phys. Radium* **1937**, *8*, 397−409.
(35) Ditchfield, R. *Mol. Phys.* **1974**, *27*, 789.
(36) Wolinski, K.; Hinton, J. F.; Pulay, P. *J. Am. Chem. Soc.* **1990**, *112*, 8251−8260.
(37) Zienau, J.; Kussmann, J.; Koziol, F.; Ochsenfeld, C. *Phys. Chem. Chem. Phys.* **2007**, *9*, 4552−4562.
(38) Zienau, J.; Kussmann, J.; Ochsenfeld, C. *Mol. Phys.* **2010**, *108*, 333−342.
(39) Polkowska, J.; Bastkowski, F.; Schrader, T.; Klärner, F.-G.; Zienau, J.; Koziol, F.; Ochsenfeld, C. *J. Phys. Org. Chem.* **2009**, *22*, 779−790.
(40) Flaig, D.; Beer, M.; Ochsenfeld, C. *J. Chem. Theory Comput.* **2012**, *8*, 2260−2271.
(41) Ochsenfeld, C.; Kussmann, J.; Koziol, F. *Angew. Chem., Int. Ed.* **2004**, *43*, 4485−4489.
(42) Kussmann, J.; Ochsenfeld, C. *J. Chem. Phys.* **2007**, *127*, 054103.
(43) Beer, M.; Ochsenfeld, C. *J. Chem. Phys.* **2008**, *128*, 221102.
(44) Beer, M.; Kussmann, J.; Ochsenfeld, C. *J. Chem. Phys.* **2011**, *134*, 074102.
(45) Weigend, F.; Ahlrichs, R. *Phys. Chem. Chem. Phys.* **2005**, *7*, 3297.
(46) (a) Bühl, M.; Mauschick, F. T. *Phys. Chem. Chem. Phys.* **2002**, *4*, 5508−5514. (b) Bühl, M.; Parrinello, M. *Chem.—Eur. J.* **2001**, *7*, 4487−4494.
(47) Pennanen, T. S.; Vaara, J.; Lantto, P.; Sillanpää, A. J.; Laasonen, K.; Jokisaari, J. *J. Am. Chem. Soc.* **2004**, *126*, 11093−11102.
(48) Kongsted, J.; Nielsen, C. B.; Mikkelsen, K. V.; Christiansen, O.; Ruud, K. *J. Chem. Phys.* **2007**, *126*, 034510−1−034510−8.
(49) (a) Aidas, K.; Møgelhøj, A.; Nielsen, C. B.; Mikkelsen, K. V.; Ruud, K.; Christiansen, O.; Kongsted, J. *J. Phys. Chem. A* **2007**, *111*, 4199−4210. (b) Aidas, K.; Mikkelsen, K. V.; Kongsted, J. *Phys. Chem. Chem. Phys.* **2009**, *12*, 761−768.
(50) Bulo, R. E.; Jacob, C. R.; Visscher, L. *J. Phys. Chem. A* **2008**, *112*, 2640−2647.
(51) (a) Klärner, F.-G; Panitzky, J.; Bläser, D.; Boese, R. *Tetrahedron* **2001**, 3673−3687. (b) Klärner, F.-G.; Polkowska, J.; Panitzky, J.; Seelbach, U. P.; Burkert, U.; Kamieth, M.; Baumann, M.; Wigger, A. E.; Boese, R.; Blaeser, D. *Eur. J. Org. Chem.* **2004**, *7*, 1405−1423.
(52) Gallivan, J. P.; Dougherty, D. A. *J. Am. Chem. Soc.* **2000**, *122*, 870−874.
(53) Ruloff, R.; Seelbach, U. P.; Merbach, A. E.; Klärner, F.-G. *J. Phys. Org. Chem.* **2002**, *15*, 189−196 and references therein.